Angewandte Chemie International Edition

Iron Fluorides

DOI: 10.1002/anie.201206464

A Matrix-Isolation and Quantum-Chemical Investigation of FeF_4**

*Tobias Schlöder, Thomas Vent-Schmidt, and Sebastian Riedel**

Iron is the second most abundant metal in the earth's crust, and owing to this high natural abundance it can be considered as one of the most important elements. Chemically it plays an important role in the active sites of many enzymes and it is therefore given increasing attention as a cheap, non-toxic, and environmentally friendly alternative in organic catalysis.[1] In both enzymatic and artificial catalytic reactions, oxidation and reduction processes are crucial. The most abundant oxidation states of iron are $+2$ and $+3$, but higher oxidation numbers up to $+6$ are experimentally known.[2] These higher oxidation states of iron are usually stabilized by oxygen, for example in the tetraoxoferrate(VI) anion $[FeO_4]^{2-}$, of which several salts are known.[3] Beyond these anionic complexes, neutral iron oxides, such as $[O_2Fe(\eta^2\text{-}O_2)]$, have been stabilized under cryogenic conditions in rare gas matrices.[4] Furthermore, iron nitrido complexes in the $+5$ and $+6$ oxidation states have been successfully prepared in solution at low temperatures, as shown by Mössbauer and X-ray absorption spectroscopy.[5,6]

Despite a long history of research in this field, only a few binary iron halides are known.[7] Both FeF_2 and FeF_3 are well-known and intensively studied compounds,[8–11] whereas the next in line, FeF_4, has so far eluded unambiguous identification. In a combined mass-spectrometric and matrix-isolation investigation, FeF_3 was reacted with the fluorine atom donor CeF_4, and the existence of FeF_4 has been postulated based on the relative abundance of $[FeF_3]^+$ and $[FeF_2]^+$ fragments in the mass spectrum and a new weak IR absorption at 758.5 cm^{-1} in an argon matrix, which could not be assigned to one of the lower fluorides.[12] As no other related band was observed, FeF_4 was assumed to have a highly symmetric, either square-planar or tetrahedral structure, which is highly improbable for a d^4 system for which a Jahn–Teller distortion is to be expected. Furthermore, no quantum-chemical calculations were made to support the assignment of the band or the suggested structure.[12]

Herein, we present the IR spectra of matrix-isolated iron tetrafluoride combined with state-of-the-art quantum-chemical calculations, which strongly support our interpretation of the spectra.

Laser-ablated iron atoms were codeposited with elemental fluorine under excess argon or neon onto a KBr or CsI window cooled to 10.0 and 3.8 K, respectively, for deposition. The IR spectra directly after deposition as well as after additional annealing to slightly higher temperatures are shown in Figure 1 for a neon and an argon matrix.

Directly after deposition, three major groups of absorptions can be observed, two of which have previously been assigned to FeF_2 and FeF_3 (see Figure 1),[13–15] whereas the third band at higher wavenumbers was previously unknown. Beyond these iron fluorides, the absorptions of the $[F_3]^-$ anion typically generated in this kind of laser-ablated experiments can also be seen (510.2 cm^{-1} in argon and 524.8 cm^{-1} in neon, see Figure 2).[16]

The additional band at 778.6 cm^{-1}, observed in neon matrices, is relatively strong directly after sample deposition. Annealing of the neon matrix to 9.0 K slightly reduces the intensities of the 752.5 and 743.6 cm^{-1} bands of FeF_2 and FeF_3, whereas the new 778.6 cm^{-1} band increases, (Figure 1, Ne (c)). Irradiation of the neon matrix using the full spectra of a mercury arc lamp leads to a decrease of the 778.6 cm^{-1} band and an increase of the corresponding FeF_2 and FeF_3 bands (Figure 1, Ne (e)). Based on our state-of-the-art quantum-chemical calculations, we assign this new band at 778.6 cm^{-1} to the FeF_4 molecule, which is formed by the reaction between F_2 molecules and adjacent iron atoms or lower fluorides and decomposes upon irradiation $\lambda > 220$ nm to FeF_2 and FeF_3 (Figure 1, Ne). Further photolyzation experiments with different high-pass filter showed that FeF_4 only decomposes when being irradiated with UV radiation with a wavelength of $\lambda < 320$ nm (Supporting Information, Figure SI2).

Owing to the Jahn–Teller distortion in FeF_4, a second IR-active iron–fluorine stretching vibration is expected (see below). In the spectra obtained from the neon matrices, a very weak band was indeed observed at 656.7 cm^{-1} (Figure 2).

In argon matrices, the new line only grows after annealing to 30 K as a broader band centered at 757 cm^{-1}. Unfortunately, the second absorption, which was identified in neon, could not be observed in argon. This is most likely due the large width of the corresponding band. All attempts to reduce the broadness of the band in argon matrices have so far failed. Nevertheless, the difference spectrum in Figure 1, Ar (c) undoubtedly shows the increase of the 757 cm^{-1} band upon decrease of the 730.5 cm^{-1} and 728.5 cm^{-1} bands of FeF_2 and FeF_3 indicating an oxidation of the lower fluorides and the formation of FeF_4.

---

[*] T. Schlöder, T. Vent-Schmidt, Dr. S. Riedel
Albert-Ludwigs-Universität Freiburg
Institut für Anorganische und Analytische Chemie
Albertstrasse 21, 79104 Freiburg (Deutschland)
E-mail: sebastian.riedel@psichem.de
Homepage: http://www.psichem.de

[**] This work has been supported by the DFG project HA 5639/3-1 and the Fonds der Chemischen Industrie (FCI). We are grateful to the BWGrid cluster for providing computational resources and to Dr. Eicher from the Solvay Fluor GmbH for generous support with F_2. We thank C. Roll, R. Tomm, and M. Melder from the technical workshop of the chemistry department for their help with the construction of the matrix chamber and the laser-ablation setup. We are also grateful to Prof. Ingo Krossing and Prof. Harald Hillebrecht for their generous and continuous support.

Supporting information for this article is available on the WWW under http://dx.doi.org/10.1002/anie.201206464.

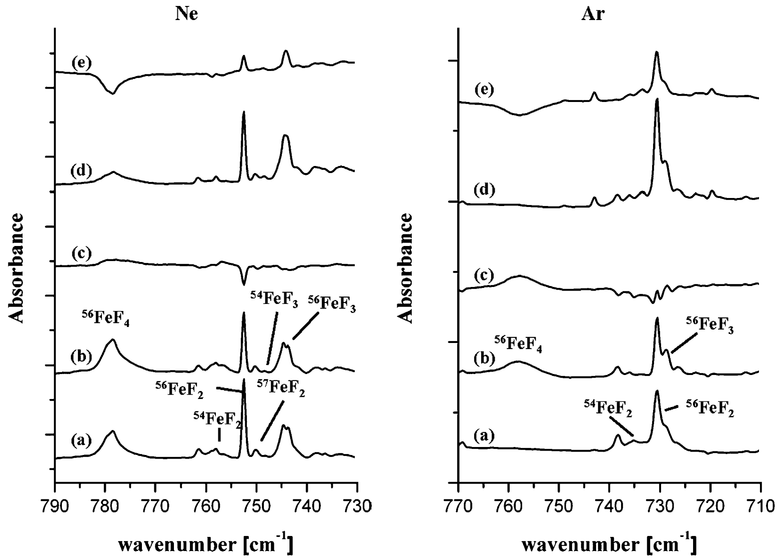

Figure 1. IR spectra in the 730–790 cm^{-1} region (Ne) and the 710–770 cm^{-1} region (Ar) obtained after co-deposition of laser-ablated iron atoms with $\mathrm{F_2}$ in excess of the respective noble gas. a) After 1 h of sample deposition at 3.8 K (Ne) and 10.0 K (Ar). b) After annealing to 9 K (Ne) and 30 K (Ar). c) Difference spectrum (spectrum measured after annealing minus spectrum directly after deposition). d) After irradiation $\lambda > 220$ nm. e) Difference spectrum (spectrum measured after irradiation minus spectrum after annealing).

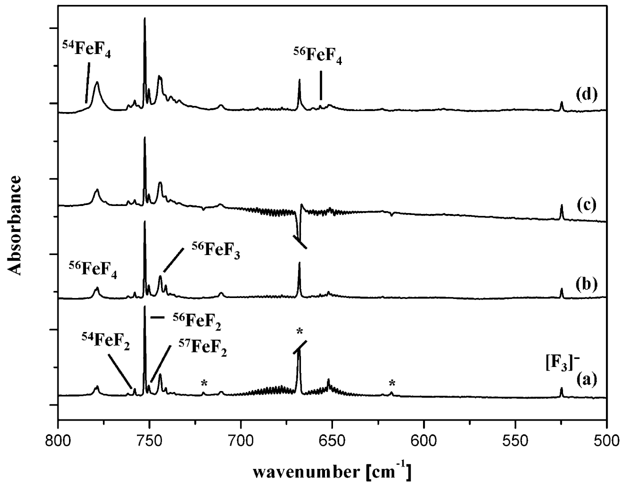

Figure 2. Infrared spectra in the 500–800 cm^{-1} region obtained after co-deposition of laser-ablated iron atoms with $\mathrm{F_2}$ in excess neon (*gas phase $\mathrm{CO_2}$ bands). a) After 1 h of sample deposition at 3.8 K using 0.5% $\mathrm{F_2}$. b)–d) As in (a) but with b) 1% $\mathrm{F_2}$, c) 2% $\mathrm{F_2}$, d) 3% $\mathrm{F_2}$.

When the fluorine concentration is increased from 0.5 to 3% in Ne (see Figure 2) or Ar (Supporting Information, Figure SI1), the intensity of the $\mathrm{FeF_4}$ clearly increases. The major difference between the neon and argon experiments is that $\mathrm{FeF_4}$ is immediately formed after sample deposition when neon is used as the matrix host, whereas the corresponding band in the argon matrices only appears after annealing to 30 K.

To unambiguously identify the reaction products by IR spectroscopy (Table 1), we performed structure optimizations and harmonic as well as anharmonic frequency analyses of binary iron fluoride molecules using density functional theory and ab initio methods up to the CCSD(T) level. The energy minimized structures are shown in Figure 3.

Table 1: Observed IR absorptions obtained after co-deposition of laser-ablated iron atoms with elemental fluorine in excess noble gases.[a]

Compound	Neon	Argon	References
^{57}FeF$_2$	750.0	–	pw
^{56}FeF$_2$	752.5	730.5	pw
^{56}FeF$_2$	752.8	731.3	[13]
^{54}FeF$_2$	758.0	736.1	pw
^{56}FeF$_3$	743.6/744.6	728.5	pw
^{56}FeF$_3$	743.6	728.5	[14,15]
^{54}FeF$_3$	748.3	–	pw
^{56}FeF$_4$	651.9	–	pw
^{56}FeF$_4$	778.6	757	pw
^{54}FeF$_4$	784.4	763	pw

[a] Values in cm^{-1}. pw = present work.

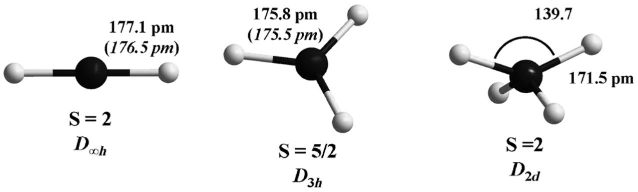

Figure 3. Equilibrium structures of molecular iron fluorides calculated at the CCSD(T)/aVTZ level. Values in parentheses were obtained using the awCVTZ-NR basis set for iron.

$\mathrm{FeF_2}$ and $\mathrm{FeF_3}$ are both well-known molecules of $D_{\infty h}$ and D_{3h} symmetries, respectively, which exist in their high-spin ground states ($^5\Delta_g$ and $^6A_1'$, respectively). The calculated equilibrium bond lengths at the CCSD(T)/aVTZ level are 177.1 pm for $\mathrm{FeF_2}$ and 175.8 pm for $\mathrm{FeF_3}$. Consideration of core–valence (cv) correlation using the awCVTZ-NR basis set for iron leads to a slightly shorter bond length of $\mathrm{FeF_3}$ ($d_{\text{Fe–F}} = 175.5$ pm, $\Delta d_{\text{Fe-F}} = 0.3$ pm), whereas for $\mathrm{FeF_2}$ the cv effect is larger ($d_{\text{Fe-F}} = 176.5$ pm, $\Delta d_{\text{Fe-F}} = 0.6$ pm). The effective rotationally and vibrationally averaged internuclear distances r_g were determined experimentally by GED diffraction experiments.[10,11] The calculated r_g values are slightly longer than the experimental values, but nevertheless the agreement is good (Table 2). It can be further improved if larger basis sets are used and relativistic effects are considered.[9] Still, despite the small deviations of the bond lengths, the experimental wavenumber values are excellently reproduced by our calculations (see below). The structure optimization of $\mathrm{FeF_4}$ in its quintet high-spin state yielded a flattened tetrahedral structure (D_{2d} symmetry, electronic state ^{5}E) and, as expected, not a higher symmetrical structure. Thus, the initial presumption of a square planar or a regular tetrahedral structure

Table 2: Calculated and experimental structural parameters.[a]

Molecule	B3LYP[b]	MP2[b]	CCSD(T)[b]	CCSD(T)[c]	CCSD(T)[d]	Exp.
FeF_2 ($D_{\infty h}$, $^5\Delta_g$)	176.2	177.8	177.1 *178.8*	176.7 *178.4*	176.5 *178.2*	*176.9(4)*
FeF_3 (D_{3h}, $^6A_1'$)	176.4	175.9	175.8 *177.3*	175.6 *177.1*	175.5	*176.3(4)*
FeF_4[e] (D_{2d}, ^5E)	171.9 (138.5)	170.9 (140.2)	171.5 (139.7)	171.3 (139.4)		

[a] Bond lengths [pm] and angles [°]. Values in italics are effective, rotationally and vibrationally averaged r_g values at 1050 K for FeF_2 and 1260 K for FeF_3. [b] aVTZ basis set for Fe and F. [c] aVTZ basis set for F and wCVTZ-NR basis set for Fe. [d] aVTZ basis set for F and awCVTZ-NR basis set for Fe. [e] Values in parentheses correspond to the angle F-Fe-F(*trans*).

derived from the observation of only one IR absorption in the region of the iron–fluorine stretching modes is doubtful.

Harmonic frequencies were calculated at different levels of theory up to the coupled-cluster level. Furthermore, anharmonic corrections (VPT2) were considered at MP2 and CCSD(T) level. For FeF_2, the calculated anharmonic frequency computed at the CCSD(T)/aVTZ level is 9.8 cm^{-1} too low when compared with the experimental value in neon matrices. The agreement can be increased to a difference of 2.1 cm^{-1} if cv correlation effects are considered using the awCVTZ-NR basis set of iron. Note that the calculated frequency at CCSD(T)/aVTZ level of FeF_3 is already in very good agreement with experiment (Table 3 and the Supporting Information).

This observation correlates well with the calculated bond lengths, because cv correlation was more important for the former case than for the latter. As expected, the frequency analysis for FeF_4 shows two distinct IR-active iron–fluorine stretching modes at 779.0 (E) and 650.9 cm^{-1} (B_2) at CCSD(T)/aVTZ level. Here, the anharmonic corrections have been calculated at MP2 level, as they are very similar to those obtained at CCSD(T) level for the lower fluorides. Nevertheless, our computed frequencies agree excellently with the bands determined in neon matrices ($\Delta\nu$ (B_2 mode) = 3.5 cm^{-1} and $\Delta\nu$ (E mode) = 0.2 cm^{-1}). Furthermore, the broad $^{56}FeF_4$ absorption shows a shoulder at 784.4 cm^{-1}, which can be assigned to the $^{54}FeF_4$ isotopic band, leading to an isotopic shift of 5.8 cm^{-1}, in excellent agreement with the calculated value and additionally confirming the characterization of FeF_4 (Table 3). The shoulder corresponding to the $^{54}FeF_4$ isotopomer is also observed in the argon experiments (763 cm^{-1}; Supporting Information, Figure SI1, inset).

To put these experimental observations of FeF_4 at cryogenic conditions into perspective, the thermochemical stability of this compound was also analyzed. Three possible decomposition channels for iron tetrafluoride were taken into account: the concerted elimination of F_2 as well as the homolytic bond breaking of one iron–fluorine bond, and the corresponding bimolecular reaction. The results, which are summarized and compared to those of FeF_3 in Table 4, show only substantial endothermic decomposition energies for FeF_4.

Table 4: Calculated thermochemistry of FeF_4 and FeF_3 at different levels of theory.[a]

Reaction	B3LYP/aVTZ		MP2/aVTZ		CCSD(T)/aVTZ	
	$\Delta E^{0K[b]}$	ΔG^0	$\Delta E^{0K[b]}$	ΔG^0	$\Delta E^{0K[b]}$	ΔG^0
$FeF_4 \rightarrow FeF_2 + F_2$	369.5	330.9	297.6	264.8	317.8	289.6
$FeF_4 \rightarrow FeF_3 + F$	194.9	156.6	87.1	49.4	116.0	78.7
$FeF_4 \rightarrow FeF_3 + {}^1/_2\,F_2$	120.4	97.3	33.1	16.5	42.5	23.2
$FeF_3 \rightarrow FeF_2 + F$	323.6	292.9	312.7	281.3	348.8	322.0
$FeF_3 \rightarrow FeF_2 + {}^1/_2\,F_2$	249.1	233.6	261.8	248.3	275.3	266.4

[a] Values in $kJ\,mol^{-1}$. [b] Values are corrected for ZPE.

The most probable decomposition pathway computed at the CCSD(T)/aVTZ level is the bimolecular elimination of F_2, requiring 42.5 $kJ\,mol^{-1}$ at 0 K. Although FeF_4 is, as expected, computed to be less stable than FeF_3, it still shows only endergonic decomposition channels at standard conditions, at least if only gas-phase species are considered (see Table 4). To evaluate the possible existence of iron tetrafluoride as bulk material, a Born–Fajans–Haber cycle starting from solid FeF_3 and elemental fluorine was constructed (Scheme 1). The Gibbs standard sublimation enthalpy of FeF_3 was taken from literature[17] and the Gibbs reaction enthalpy for the gas-phase reaction was calculated at the CCSD(T)/aVTZ level. The result indicates that a minimum of $\Delta_{sub}G(FeF_4) = 136.4\ kJ\,mol^{-1}$ would be needed to be released upon condensation of gaseous FeF_4 if the compound were stable as bulk material. For an estimation of the sublimation enthalpies of FeF_4, we applied a previous

Table 3: Calculated and observed wavenumbers [cm^{-1}] of the Fe–F stretching modes of molecular iron fluorides.

Mol.[a]	(Mode)	CCSD(T)[b]	CCSD(T)[c]	CCSD(T)[d]	Ne	Ar
FeF_2 (Σ_u^-)	ν[e]	742.7	747.4	750.4	752.5	730.5
	^{56}Fe[f]	751.8	756.2	759.4		
	^{54}Fe[f]	757.4	761.8	765.1	758.0	736.1
	$\Delta\nu_{iso}$	5.6	5.6	5.7	5.5	5.6
FeF_3 (E')	ν[e]	742.8	744.4	–	743.6	728.5
	^{56}Fe[f]	751.2	753.4	755.1		
	^{54}Fe[f]	756.0	758.2	759.9	748.3	–
	$\Delta\nu_{iso}$	4.8	4.8	4.8	4.7	–
FeF_4 (B_2)	ν[g]	650.9	656.9	–	656.7	–
	^{56}Fe[f]	660.0	665.6	–		
	^{54}Fe[f]	661.5	667.1	–	–	–
	$\Delta\nu_{iso}$	1.5	1.4	–	–	–
FeF_4 (E)	ν[f]	779.0	782.1	–	778.6	757
	^{56}Fe[f]	791.4	794.4	–		
	^{54}Fe[f]	797.2	800.2	–	784.4[h]	763[h]
	$\Delta\nu_{iso}$	5.8	5.8	–	5.8	6

[a] Symmetry labels are those for the corresponding stretching modes. [b] aVTZ basis set for Fe and F. [c] aVTZ basis set for F and wCVTZ-NR basis set for Fe. [d] aVTZ basis set for F and awCVTZ-NR basis set for Fe. [e] Anharmonic corrected frequesncies. [f] Harmonic frequency calculations using the ^{56}Fe or ^{54}Fe isotope. [g] Anharmonic corrected frequencies using MP2 anharmonic values. [h] Shoulder.

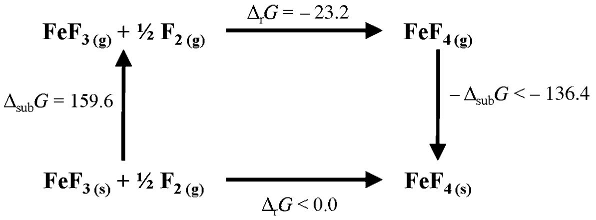

Scheme 1. Born–Fajans–Haber cycle for the formation of solid FeF_4 under standard conditions. Values are in $kJ\,mol^{-1}$.

method[18] and obtained an estimated value of $\Delta_{sub}H(FeF_4) \approx 135\,kJ\,mol^{-1}$. However, the entropic contribution, which amounts to $61.4\,kJ\,mol^{-1}$ for FeF_3, needs to be taken into account and it is thus unlikely that FeF_4 is a stable compound in the condensed phase.

In conclusion, matrix-isolation experiments in neon and argon clearly show IR absorptions that are consistent with the formation of a higher iron fluoride beyond FeF_3. The new IR bands observed in neon (778.3 and $656.7\,cm^{-1}$) and argon matrices ($757\,cm^{-1}$) can unambiguously be assigned to the new binary iron tetrafluoride owing to the excellent agreement between the calculated wavenumbers and the experimental values using neon as the matrix host. With increasing fluorine concentration, the intensity of the band corresponding to FeF_4 increases. Furthermore, the computed and experimental isotopic shifts of $^{56}FeF_4/^{54}FeF_4$ further support this assignment. The present findings support the previous tentative assignment of the $758.5\,cm^{-1}$ argon matrix band to a higher iron fluoride.[12] Although the FeF_4 molecule is computed to be stable in the gas phase under standard conditions, its existence as bulk material seems improbable, as shown by a Born–Fajans–Haber cycle. Nevertheless, it might be stabilized in *a*HF solutions, but the calculation of solvation energies are beyond the scope of the present study.

Experimental Section

Matrix-isolation experiments: Argon (99.999 %, Sauerstoffwerk Friedrichshafen) and neon (99.999 %, Air Liquide) were stored in glass bulbs, and F_2 (99.8 %, Solvay) in a stainless steel cylinder cooled to 77 K during the experiments to freeze out impurities. The gas storage vessels were connected to a self-made matrix chamber by a stainless steel capillary. The reactants were condensed onto KBr and CsI windows cooled to 3.8 K (neon) or 10.0 K (argon) using a closed-cycle helium cryostat (Sumitomo Heavy Industries, RDK-205D) inside the vacuum chamber. For the laser-ablation experiments, the 1064 nm fundamental of a Nd:YAG laser (Continuum, Minilite II, 10 Hz repetition rate and 6 ns pulse width) was used which was focused onto a rotating iron target (99.9 %, Strem chemicals) through a hole in the cold window. Matrix samples have been prepared by the laser-ablation process of iron atoms together with co-deposited F_2 (different concentrations ranging from 0.5 to 3 %) under excess of rare gas for 1 h. The infrared spectra were recorded on a Bruker Vertex 70 spectrometer purged with dry air at $0.5\,cm^{-1}$ resolution in the region between 4000 and $450\,cm^{-1}$ using a RT-DLaTGS and liquid nitrogen cooled MCT detector. The matrix samples were irradiated by a mercury arc street lamp (Osram HQL 250) with the outer globe removed.

Quantum-chemical calculations: The structures of all molecules have been fully optimized (by relaxing all parameters) at density functional theory level using the B3LYP[19–21] hybrid functional and Dunning's correlation consistent triple-ζ basis set for Fe and F (aug-cc-pVTZ, for brevity denoted as aVTZ).[22,23] All possible spin multiplicities have been considered. Structure optimizations at ab-initio levels (MP2 and CCSD(T)) have then been performed for the ground states of all molecules within the restrictions of their respective point groups. To evaluate the influence of the core–valence contributions, several triple-ζ basis sets of iron have been used (aug-cc-pVTZ, cc-pwCVTZ and aug-cc-pwCVTZ).[22] Harmonic and anharmonic frequency calculations were carried out for stationary points on the potential energy surface for both ^{56}Fe and ^{54}Fe isotopes. For the DFT and ab initio calculations, the Gaussian 03[19] and CFOUR[24] program packages, respectively, were used.

Received: August 10, 2012

Keywords: coupled-cluster calculations · fluorine · IR spectroscopy · iron · matrix-isolation experiments

[1] E. B. Bauer, *Curr. Org. Chem.* **2008**, *12*, 1341.
[2] S. Riedel, M. Kaupp, *Coord. Chem. Rev.* **2009**, *253*, 606.
[3] W. Levason, C. A. McAuliffe, *Coord. Chem. Rev.* **1974**, *12*, 151.
[4] Y. Gong, M. Zhou, L. Andrews, *J. Phys. Chem. A* **2007**, *111*, 12001.
[5] J. J. Scepaniak, C. S. Vogel, M. M. Khusniyarov, F. W. Heinemann, K. Meyer, J. M. Smith, *Science* **2011**, *331*, 1049.
[6] J. F. Berry, E. Bill, E. Bothe, G. S. DeBeer, B. Mienert, F. Neese, K. Wieghardt, *Science* **2006**, *312*, 1937.
[7] A. F. Holleman, E. Wiberg, *Lehrbuch der Anorganischen Chemie*, *Vol. 102*, Walter de Gruyter, Berlin, **2007**.
[8] V. G. Solomonik, J. F. Stanton, J. E. Boggs, *J. Chem. Phys.* **2005**, *122*, 094322.
[9] V. G. Solomonik, J. F. Stanton, J. E. Boggs, *J. Chem. Phys.* **2008**, *128*, 244104.
[10] M. Hargittai, M. Kolonits, J. Tremmel, *Struct. Chem.* **1990**, *1*, 75.
[11] N. Vogt, *J. Mol. Struct.* **2001**, *570*, 189.
[12] J. V. Rau, S. Nunziante Cesaro, N. S. Chilingarov, M. S. Leskiv, G. Balducci, L. N. Sidorov, *Inorg. Chem. Commun.* **2003**, *6*, 643.
[13] J. W. Hastie, R. H. Hauge, J. L. Margrave, *J. Chem. Soc. D* **1969**, 1452.
[14] S. B. Osin, D. I. Davliatshin, J. S. Ogden, *J. Fluorine Chem.* **1996**, *76*, 187.
[15] Y. B. Predtechenskii, L. D. Shcherba, in *Proceedings of the 12th All-Union Symposium*, Minsk, USSR, **1989**.
[16] S. Riedel, T. Köchner, X. Wang, L. Andrews, *Inorg. Chem.* **2010**, *49*, 7156.
[17] M. W. Chase, Jr., *NIST-JANAF Themochemical Tables*, 4th ed., **1998**.
[18] M. V. Korobov, L. N. Savinova, L. N. Sidorov, *J. Chem. Thermodyn.* **1993**, *25*, 1161.
[19] Gaussian 03, Revision C.02, M. J. Frisch, G. W. Trucks, H. B. Schlegel, G. E. Scuseria, M. A. Robb, J. R. Cheeseman, J. A. Montgomery, Jr., T. Vreven, K. N. Kudin, J. C. Burant, J. M. Millam, S. S. Iyengar, J. Tomasi, V. Barone, B. Mennucci, M. Cossi, G. Scalmani, N. Rega, G. A. Petersson, H. Nakatsuji, M. Hada, M. Ehara, K. Toyota, R. Fukuda, J. Hasegawa, M. Ishida, T. Nakajima, Y. Honda, O. Kitao, H. Nakai, M. Klene, X. Li, J. E. Knox, H. P. Hratchian, J. B. Cross, V. Bakken, C. Adamo, J. Jaramillo, R. Gomperts, R. E. Stratmann, O. Yazyev, A. J. Austin, R. Cammi, C. Pomelli, J. W. Ochterski, P. Y. Ayala, K. Morokuma, G. A. Voth, P. Salvador, J. J. Dannenberg, V. G. Zakrzewski, S. Dapprich, A. D. Daniels, M. C. Strain, O. Farkas, D. K. Malick, A. D. Rabuck, K. Raghavachari, J. B. Foresman, J. V. Ortiz, Q. Cui, A. G. Baboul, S. Clifford, J. Cioslowski, B. B. Stefanov, G. Liu, A. Liashenko, P. Piskorz, I. Komaromi, R. L. Martin, D. J. Fox, T. Keith, M. A. Al-Laham, C. Y. Peng, A.

Nanayakkara, M. Challacombe, P. M. W. Gill, B. Johnson, W. Chen, M. W. Wong, C. Gonzalez, J. A. Pople, Gaussian, Inc., Wallingford CT, **2004**.

[20] A. D. Becke, *J. Chem. Phys.* **1993**, *98*, 5648.

[21] C. Lee, W. Yang, R. G. Parr, *Phys. Rev. B* **1988**, *37*, 785.

[22] N. B. Balabanov, K. A. Peterson, *J. Chem. Phys.* **2005**, *123*, 064107.

[23] T. H. Dunning, Jr., *J. Chem. Phys.* **1989**, *90*, 1007.

[24] J. F. Stanton, J. Gauss, M. E. Harding, P. G. Szalay, A. A. Auer, R. J. Bartlett, U. Benedikt, C. Berger, D. E. Bernholdt, Y. J. Bomble, O. Christiansen, M. Heckert, O. Heun, C. Huber, T.-C. Jagau, D. Jonsson, J. Jusélius, K. Klein, W. J. Lauderdale, D. A. Matthews, T. Metzroth, D. P. O'Neill, D. R. Price, E. Prochnow, K. Ruud, F. Schiffmann, S. Stopkowicz, A. Tajti, J. Vázquez, F. Wang, J. D. Watts, CFour 1.2 ed., Mainz, **2010**.